

GADOLINIUM BOROSILICATE GLASS-BONDED Gd-SILICATE APATITE: A GLASS-CERAMIC NUCLEAR WASTE FORM FOR ACTINIDES

Donggao Zhao*, Liyu Li**, L.L. Davis**, W.J. Weber**, R.C. Ewing*

*Department of Nuclear Engineering & Radiological Sciences, University of Michigan, Ann Arbor, Michigan 48109-2104

**Pacific Northwest National Laboratory, Richland, Washington 99352

ABSTRACT

A Gd-rich crystalline phase precipitated in a sodium gadolinium alumino-borosilicate glass during synthesis. The glass has a chemical composition of 45.4-31.1 wt % Gd_2O_3 , 28.8-34.0 wt % SiO_2 , 10.8-14.0 wt % Na_2O , 4.3-5.9 wt % Al_2O_3 , and 10.8-14.9 wt % B_2O_3 . Backscattered electron images revealed that the crystals are hexagonal, elongated, acicular, prismatic, skeletal or dendritic, tens of μm in size, some reaching 200 μm in length. Electron microprobe analysis confirmed that the crystals are chemically homogeneous and have a formula of $NaGd_9(SiO_4)_6O_2$ with minor B substitution for Si. The X-ray diffraction pattern of this phase is similar to that of lithium gadolinium silicate apatite. Thus, this hexagonal phase is a rare earth silicate with the apatite structure. We suggest that this Gd-silicate apatite in a Gd-borosilicate glass is a potential glass-ceramic nuclear waste form for actinide disposition. Am, Cm and other actinides can easily occupy the Gd-sites. The potential advantages of this glass-ceramic waste form include: 1) both the glass and apatite can be used to immobilize actinides, 2) silicate apatite is thermodynamically more stable than the glass, 3) borosilicate glass-bonded Gd-silicate apatite is easily fabricated, and 4) the Gd is an effective neutron absorber.

INTRODUCTION

Considerable effort has been devoted to determining distributions and solubility limits of radionuclides and neutron absorbers in borosilicate glasses in the four-component $Na_2O-B_2O_3-Al_2O_3-SiO_2$ system [1-3]. In recent years, glass compositions in this system have been developed to test the effects of changing compositions on the solubilities of the neutron absorbers Gd and Hf [1-3]. When Gd exceeds its solubility limit in the glass during synthesis of Gd-borosilicate glasses, a Gd-rich crystalline silicate phase precipitates. Likewise, Gd-rich crystalline silicate phases precipitate in Gd-borosilicate glasses during extended times at elevated temperatures [4], as would occur during slow cooling of canisters or during repository storage. The purpose for synthesizing a Gd-borosilicate glass is to incorporate as much Gd as possible into the glass. Therefore, the precipitation of a Gd-rich crystalline phase from the glass matrix was initially considered unwanted. However, as a Gd-rich phase, this crystalline phase may also immobilize actinides, as has been demonstrated previously [4]. An essential issue of the long-term immobilization and disposal of actinides is whether a waste form is sufficiently durable. Durability may be based on a variety of chemical and physical properties, e.g., mechanical strength, thermodynamic stability, slow kinetics of corrosion, or low diffusivity of radionuclides and neutron absorbers. Durable phases that survive weathering, erosion, transport, and deposition over geologic periods are potential candidates for actinide waste forms. Such phases include zircon, $ZrSiO_4$, calcium phosphate apatite, $Ca_{4-x}REE_{6+x}(SiO_4)_{6-y}(PO_4)_y(O,F)_2$, monazite, $(Ce,La,Nd,Th)PO_4$, pyrochlore, $(Ca,REE)_2Ti_2O_6(OH,F)$, zirconolite, $(Ca,Th,Ce)Zr(Ti,Nb)_2O_7$, baddeleyite, ZrO_2 , and zirconia, ZrO_2 [1, 4, 5].

In this paper, we characterize the Gd-rich crystalline silicate phase in terms of its chemistry, structure and susceptibility to radiation damage and propose Gd-silicate in a Gd-borosilicate glass matrix as a possible glass-ceramic nuclear waste form for actinides. A variety of other

Gd-bearing silicates have been reported previously. These Gd-silicates include digadolinium silicate oxide Gd_2SiO_5 [6], gadolinium disilicate $\text{Gd}_2\text{Si}_2\text{O}_7$ [7-8], gadolinium silicate oxide $\text{Gd}_{14}\text{Si}_9\text{O}_{39}$ [9], lithium gadolinium oxide silicate $\text{LiGd}_9\text{Si}_6\text{O}_{26}$ [10], sodium gadolinium silicate NaGdSiO_4 [11], sodium gadolinium silicate hydroxide $\text{NaGdSiO}_4(\text{NaOH})_{0.213}$ [12], sodium gadolinium tecto-alumosilicate hydrate $\text{Na}_7\text{Gd}_{27}(\text{Al}_{88.11}\text{Si}_{103.9}\text{O}_{384})(\text{H}_2\text{O})_{195}$ [13], and sodium gadolinium silicate fluoride oxide $(\text{Na}_{1.19}\text{Gd}_{8.81})(\text{SiO}_4)_6(\text{F}_{0.38}\text{O}_{1.62})$ [14].

EXPERIMENT

Sample Synthesis

Sodium gadolinium silicate crystals precipitate from borosilicate glasses when Gd exceeds its solubility limits [1, 3]. The baseline borosilicate glass has a composition of $15\text{B}_2\text{O}_3 \cdot 20\text{Na}_2\text{O} \cdot 5\text{Al}_2\text{O}_3 \cdot 60\text{SiO}_2$ (mole %). Baseline glasses were synthesized in a covered Pt - 10 % Rh crucible at temperatures between 1110°C and 1400°C from well-mixed powders of SiO_2 , Al_2O_3 , H_3BO_3 and Na_2CO_3 . The borosilicate glasses were then quenched and ground to approximately 200 mesh. The glasses were melted again at 1450°C after adding Gd_2O_3 [1]. The glass melts, with varying amounts of Gd_2O_3 , were quenched by immersion of the base of the crucible in water. The resulting products are transparent, colorless sodium gadolinium borosilicate glasses; one of these glasses (B15Gd48) contained an exotic crystalline phase, a sodium gadolinium silicate apatite.

Analytical techniques

The sodium gadolinium alumino-borosilicate glass and the precipitated gadolinium silicate apatite were studied by electron microprobe analysis (EMPA), scanning electron microscopy (SEM), and X-ray powder diffraction (XRD). The EMPA and SEM work was done in the Electron Microbeam Analysis Laboratory at University of Michigan. The XRD work was done at Pacific Northwest National Laboratory and University of Michigan. Backscattered electron (BSE) images and energy dispersive X-ray spectra (EDS) were used to qualitatively identify elements in the phases. A four-spectrometer Cameca CAMEBAX electron microprobe analyzer was used to obtain chemical compositions of the glass and the crystalline precipitates. Powder X-ray diffraction was used to determine the crystal structure of the precipitated silicate apatite. The Cameca PAP correction routine $f(rz)$, i.e., modified ZAF (atomic number Z, Absorption and Fluorescence) by Pichou and Pichour [15], was used in data reduction. EMPA procedures used are given in reference [16-17]. The accelerating voltage was 20 kV; the beam current was 15 nA; and the peak and background counting times were 30 and 15 seconds, respectively. Large beam sizes, lower beam current, and a shorter counting time were used to avoid possible Na migration.

RESULTS AND DISCUSSION

Gadolinium borosilicate glass

The measured chemical compositions of the crystal-bearing sodium gadolinium alumino-borosilicate glass by EMPA are 45.39-31.13 wt % Gd_2O_3 , 28.80-34.04 wt % SiO_2 , 10.75-14.02 wt % Na_2O , 4.30-5.89 wt % Al_2O_3 , and 10.75-14.91 wt % B_2O_3 (Table I), which are heterogeneous [16]. There are two compositional domains identified in the glass host. In the BSE image (Figure 1A), the glass matrix from the darker upper left area is enriched in Si, Al and Na and depleted in Gd; whereas, the glass matrix from the brighter region is enriched in Gd (Table I). The heterogeneity of the glass matrix may be the result of crystallization that

removes Gd from the glass matrix. The differences between the target and the measured compositions are significant. The glass matrix has 31.13 wt % Gd_2O_3 in the darker areas and 45.39 wt % Gd_2O_3 in the brighter areas, both of these compositions differ from the target composition of 48.00 wt % Gd_2O_3 . The composition of the brighter areas is closest to the target composition (Table I).

Table I. Target and measured compositions (wt %) of the glass host and measured composition of the precipitated Gd-silicate apatite in sample B15Gd48

	target	bright glass domain	dark glass domain	crystal
Average		5 analyses	4 analyses	22 analyses
SiO_2	29.30	28.8 ± 0.3	34.0 ± 0.3	15.7 ± 0.2
Al_2O_3	4.14	4.3 ± 0.1	5.9 ± 0.1	0.0
Na_2O	10.07	10.8 ± 0.2	14.0 ± 0.3	1.4 ± 0.1
Gd_2O_3	48.00	45.4 ± 1.4	31.1 ± 1.1	81.6 ± 2.0
B_2O_3	8.49	10.8	14.9	1.7

Note: 1 σ analytical errors from counting statistics given for measured compositions; B_2O_3 by difference.

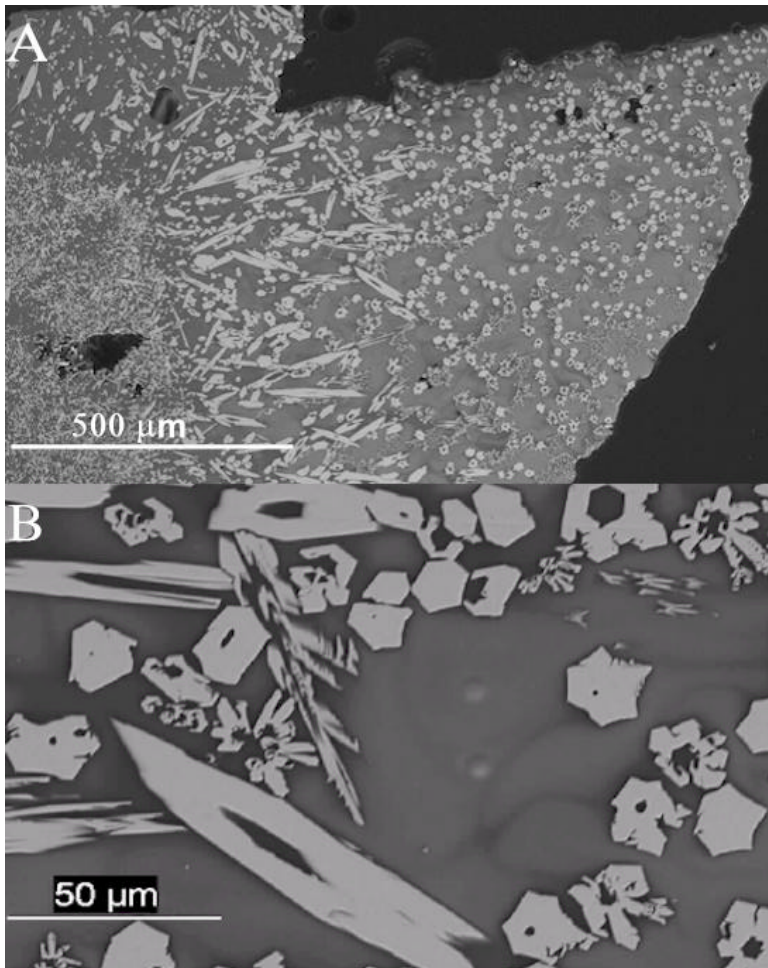


Figure 1. Backscattered electron images of the glass containing the precipitated crystalline phase in sample B15Gd48. A) Elongated, acicular, prismatic or dendritic Gd-silicate apatite crystals; cross sections are often hexagonal; glass matrix in the upper left area slightly darker than those in the central and lower right areas, indicating chemical heterogeneity of the matrix. B) Enlarged image of the central area in A. The precipitated crystals are on average tens of μm in size, but some are up to 200 μm in length.

Gd-silicate apatite

The Gd-silicate crystals that precipitated from the sodium gadolinium alumino-borosilicate glass are elongated, acicular, skeletal, prismatic or dendritic; and most crystals are tens of μm in size, but some crystals are up to 200 μm in length (Figure 1B). Cross sections of the crystals are often hexagonal, sometimes skeletal with hexagonal euhedral voids at their centers. The composition of the crystals was obtained from EMPA and tabulated in Table I. The electron microprobe analyses obtained during three analytical sessions were the same, although they were obtained with different beam sizes. Na_2O contents of the precipitated crystals were the same when analyzed using different electron beam sizes (from a point beam to a $15 \times 15 \mu\text{m}$ rastered beam), indicating that alkali, i.e., sodium, loss is not significant. The mean and standard deviations of the 22 analyses are: SiO_2 15.66 ± 0.30 wt %, Gd_2O_3 81.25 ± 0.81 wt %, and Na_2O 1.38 ± 0.06 wt %. The crystals of different shapes have the same composition, and each crystal is chemically homogeneous. The chemical formula of this phase based on EMPA is approximately $\text{NaGd}_9(\text{SiO}_4)_6\text{O}_2$ or $\text{NaGd}_9\text{Si}_6\text{O}_{26}$, which has the same formula as $\text{LiGd}_9\text{Si}_6\text{O}_{26}$ [10]. Some minor B may substitute for Si in the structure [16].

The powder X-ray diffraction pattern of the precipitated crystals can be indexed in the hexagonal system and is similar to that of lithium gadolinium silicate $\text{LiGd}_9\text{Si}_6\text{O}_{26}$, a rare earth silicate apatite. The latter has space group $P6_3/m$ or $P6_3$, and cell parameters $\mathbf{a} = 0.9407$ nm and $\mathbf{c} = 0.6842$ nm based on powder and single-crystal X-ray examination [10]. The chemical and structural examinations demonstrate that the precipitated crystalline phase is a rare earth silicate apatite [17-18]. These crystalline phases belong to the mixed-cation oxyapatite group [19-21]. The formula of apatite, $\text{Ca}_4\text{Ca}_6(\text{PO}_4)_6(\text{F,Cl,OH})_2$, can also be expressed as $\text{A}(\text{REE})_9(\text{SiO}_4)_6\text{O}_2$, where A (4f site), which can be Li or Na, is coordinated by nine silicate oxygens, and REE (three 4f and six 6h sites) are 4f-transition lanthanides in nine-fold (4f site) or seven-fold (6h site) coordination. If P substitutes Si in silicate apatite, the formula can also be rewritten as $\text{A}_{4-x}(\text{REE})_{6+x}(\text{SiO}_4)_{6-y}(\text{PO}_4)_y(\text{F,OH,O})_2$, where A could also be Mg, Ca, Sr, Ba, Pb and Cd.

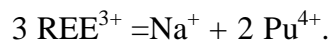
Radiation stability of silicate apatite

One of the primary concerns with crystalline Gd-silicate apatite as an actinide waste form is the radiation stability of the phase, i.e., its resistance to radiation-induced amorphization due to α -decay of actinides [22]. Radiation damage of nuclear waste forms can result in significant changes in volume, leach rate, stored energy, structure and mechanical properties [23-24]. Although radiation damage effects on this specific type of silicate apatite $\text{NaGd}_9(\text{SiO}_4)_6\text{O}_2$ have not yet been studied, a considerable number of studies are already available on radiation effects on other rare earth silicate apatites such as $\text{Ca}_3\text{Gd}_7(\text{SiO}_4)_5(\text{PO}_4)\text{O}_2$ [4, 25-26], $\text{Ca}_2\text{Nd}_8(\text{SiO}_4)_6\text{O}_2$ [27-28], $\text{Ca}_2\text{La}_8(\text{SiO}_4)_6\text{O}_2$ [29-31], and $\text{Ca}_5(\text{PO}_4)_3(\text{F,OH,Cl})$ [32]. In a study of partially devitrified Gd-borosilicate glass containing ^{244}Cm , Weber et al. [4] demonstrated that the silicate apatite, $\text{Ca}_3\text{Gd}_7(\text{SiO}_4)_5(\text{PO}_4)\text{O}_2$, formed as either small (<5 micron) or large (25 to 100 micron) crystals depending on the temperature-time history. In both cases, self-radiation damage from the decay of the ^{244}Cm resulted in the transformation of this crystalline phase to an amorphous state, which resulted in a large volume change in this phase. This large volume change resulted in microcracking within the glass in the case of large crystals; however, in the case of small crystallites, no microcracking was observed. Thus, small crystallites may be preferable. In addition, no significant changes in leach rate and mechanical properties were observed [26]. The radiation instability of the devitrification crystals, $\text{Ca}_3\text{Gd}_7(\text{SiO}_4)_5(\text{PO}_4)\text{O}_2$ [4, 25-26], and all other silicate apatites studied to date [27-32] suggests that the silicate apatite,

NaGd₉(SiO₄)₆O₂, will be sensitive to radiation-induced amorphization. While the crystalline phase NaGd₉(SiO₄)₆O₂ may be sensitive to radiation-induced amorphization, based on studies of other silicate apatites [4, 25-32], further work is required to characterize the temperature dependence (kinetics) of radiation damage of this composition, because the kinetics of radiation damage and annealing processes are known to be composition dependent [32-33]. As shown by Weber et al. [33], amorphization may not occur under repository conditions for some apatite compositions because the recovery kinetics is sufficiently high at room temperature. If this can be shown to be the case for NaGd₉(SiO₄)₆O₂, then self-radiation damage should not be an important issue.

Borosilicate glass and Gd-silicate apatite as a glass-ceramic waste form

In addition to crystalline phases and borosilicate glasses, there is a third category of waste forms, i.e., glass-ceramic or glass-bonded crystalline waste form [34-37], for example, barium aluminosilicate glass-ceramics [34], barium titanium silicate glass-ceramics [34], calcium magnesium silicate glass-ceramics [34], calcium titanium silicate glass-ceramics [35-36], phosphate apatite-based glass-ceramics [38], and glass-bonded sodalite [39]. Glass-ceramic waste forms are designed to solve the potential problem of devitrification of glass by producing a ceramic phase in a glass matrix to act as durable host for radionuclides because all glasses are thermodynamically unstable with respect to crystalline phases [40]. Glass-ceramic waste forms may offer a useful compromise between glasses and ceramics because they are easier and less expensive to prepare than conventional ceramic and have a higher durability than glass [37]. Compared with the glass matrix (Table I), the Gd-silicate crystals are greatly enriched in Gd₂O₃ (81.25 wt %) and depleted in SiO₂ (15.66 wt %) and Na₂O (1.38 wt %). In addition, the apatite structure is known to be extremely tolerant of charge-coupled cation and anion substitutions [41], as well as to cation, and probably, also anion deficiencies [19-20]. Incorporation of Pu and other actinides into the apatite structure is feasible. For example, Am³⁺, Cm³⁺, and Pu³⁺ readily enter the sites occupied by Gd because they have the same valence as Gd; thus, these actinides could be highly concentrated in the REE silicate apatite [25]. Tetravalent actinides, such as Th⁴⁺, U⁴⁺ and Pu⁴⁺, may also enter the apatite structure by coupled substitution mechanisms, such as:



The theoretical study of Meis et al. [44] also showed that both Pu³⁺ and Pu⁴⁺ could substitute for Nd. However, it has been previously demonstrated that Pu⁴⁺ in a glass does not readily substitute for Gd during the crystallization of Gd-silicate apatite, only trace quantities of Pu⁴⁺ were accommodated [25]. Thus, studies of partitioning and coupled substitutions are needed in order to determine which conditions and glass compositions (high Na or Ca) are required for the incorporation of Pu⁴⁺ at the 6h site.

Thus, the Gd-silicate apatite may be a potential actinide waste form. As a more stable phase than the borosilicate glass and with an ability to incorporate actinides, NaGd₉(SiO₄)₆O₂ may be a better waste form than the borosilicate glass host. Calcium phosphate apatite, Ca₄Ca₆(PO₄)₆(F,Cl,OH)₂, is generally durable and has been proposed as a waste form for plutonium [43]. Bros et al. [43] have demonstrated that plutonium and fissiogenic REE occur in the hydrothermal apatites from a natural nuclear reactor at the Oklo uranium deposit, located in the Franceville sedimentary basin, Gabon. ²³⁹Pu, produced by ²³⁸U epithermal neutron capture, was trapped in the apatite structure during the nuclear reactions or soon after the end of the reactions. Phosphorus-bearing silicate apatite, A_{4-x}(REE)_{6+x}(SiO₄)_{6-y}(PO₄)_y(F,OH,O)₂, is

also receiving considerable attention as an actinide waste form [1, 26, 38]. However, phosphorus-free silicate apatite of the form, $A(\text{REE})_9(\text{SiO}_4)_6\text{O}_2$, has not been considered as an actinide waste form, especially as well developed crystalline precipitates in a borosilicate glass. Contrary to most phosphate apatites proposed for immobilization of actinides, the silicate apatite proposed here has a much high Gd-content. The ability to incorporate actinides combined with its durability lead us to suggest that Gd-borosilicate glass-bonded Gd-silicate apatite is a possible glass-ceramic waste form for actinides.

There are several potential advantages using Gd-borosilicate glass-bonded Gd-silicate apatite as a glass-ceramic waste form for actinides. First, both glass matrix and crystalline apatite precipitates can be used to incorporate actinides. Second, Gd-silicate apatite precipitates are generally more durable than the glass host, thus increasing the overall durability of the waste form. Third, Gd-silicate apatite has higher thermal stability than the borosilicate glass. Finally, glass-ceramic waste forms are more tolerant of compositional variations than corresponding crystalline ceramics prepared by conventional routines and, thus, can be more easily tailored to meet specific requirements.

CONCLUSIONS

A Gd-rich crystalline silicate phase precipitates from a Gd-borosilicate glass matrix when the Gd concentration exceeds its solubility limit (11.3 mol. %) in the glass. The crystalline phase is an apatite silicate and has a composition of 81.25 wt % Gd_2O_3 , 15.66 wt % SiO_2 , 1.38 wt % Na_2O , 0.03 wt % Al_2O_3 , and 1.68 wt % B_2O_3 . The corresponding chemical formula is $\text{NaGd}_9(\text{SiO}_4)_6\text{O}_2$ or $\text{NaGd}_9\text{Si}_6\text{O}_{26}$ with minor B substitution for Si. Most crystals of the apatite silicate are tens of μm in size. X-ray diffraction data confirm that the precipitated crystals belong to the hexagonal system, and are similar to the lithium gadolinium silicate apatite, $\text{LiGd}_9\text{Si}_6\text{O}_{26}$. Radiation effects in the silicate apatite $\text{NaGd}_9(\text{SiO}_4)_6\text{O}_2$ caused by α -decay of actinides have not yet been studied. Based on studies of other silicate apatite compositions, this composition is probably sensitive to radiation-induced amorphization; however, recovery kinetics could be such as to prevent amorphization under repository conditions. Due to its thermodynamic stability, enrichment in Gd_2O_3 , and tolerance to cation and anion substitutions and deficiencies, the sodium gadolinium silicate apatite is a potential waste form for actinides. Therefore, the Gd-silicate phase and the Gd-borosilicate glass together are a potential glass-ceramic waste form for actinides.

ACKNOWLEDGMENT

This study is supported by the Environmental Management Science Program, US Department of Energy through grant # DE-FG07-97-ER45672. The electron microprobe was acquired under Grant # EAR-82-12764 from the National Science Foundation. Linda L. Davis and Denis M Strachan are thanked for their constructive comments on an early version of the manuscript.

REFERENCES

1. L. Li, D.M. Strachan, H. Li, L.L. Davis, and M. Qian, Ceramic Transaction (in press).
2. L. Li, D.M. Strachan, H. Li, L.L. Davis, and M. Qian, J. Non-Crystalline Solids (in press).
3. L.L. Davis, L. Li, J.G. Darab, H. Li, D. Strachan, P.G. Allen, J.J. Bucher, I.M. Craig, N.M. Edelstein, D.K. Shuh, Scientific Basis for Nuclear Waste Management XXII - Mat. Res. Soc. Symp. Proc., v. 556, p. 313-320 (1999).

4. W.J. Weber, R.P. Turcottte, L.R. Bunnell, F.P. Roberts, and J.H. Westsik, Jr., in: *Ceramics in Nuclear Waste Management – Proc. Int. Symp. Amer. Cer. Soc.* (eds. T.D. Chikalla and J.E. Mendel), CONF-790420, National Technical Information Service, Springfield, Virginia, p. 294-299 (1979).
5. R.C. Ewing, W. Lutze, and W.J. Weber, *J. Mater. Res.* 10, 243 (1995).
6. Y.I. Smolin and S.P. Tkachev, *Kristallografiya Krisa* 14, 22 (1969).
7. Y.I. Smolin and Y.F. Shepelov, *Izvestiya Akademii Nauk SSSR, Neorganicheskie Materialy IVNMA* 3, 1034 (1967).
8. Y.I. Smolin and Y.F. Shepelov, *Acta Crystallogr. B* 26, 484 (1970).
9. Y.I. Smolin and Y.F. Shepelov, *Izvestiya Akademii Nauk SSSR, Neorganicheskie Materialy IVNMA* 5, 1823 (1969).
10. JCPDS-ICDD # 32-0557 (1980).
11. E.I. Avetisyan, A.V. Chchagov, and N.V. Belov, *Kristallografiya Krisa* 15, 1066 (1970).
12. G.D. Fallon and B.M. Gatehouse, *Acta Crystallogr. B* 38, 919 (1982).
13. G. Calestani, G. Bacca, and G.D. Andreotti, *Zeolite* 7, 59 (1987).
14. J.M. Hughes, A.N. Mariano, and J.W. Drexler, *Neues Jb. Miner. Monat.* (7), 311 (1992).
15. G.F. Bastin, F.J.J. van Voo, and H.J.M. Heijligers, *X-ray Spectrum* 13, 91 (1984).
16. D. Zhao, L.L. Davis, L. Li, C.S. Palenik, L.M. Wang, D.M. Strachan, and R.C. Ewing, *Scientific Basis for Nuclear Waste Management - Mat. Res. Soc. Symp. Proc.* (in press).
17. D. Zhao, L.M. Wang, R.C. Ewing, L. Li, L.L. Davis, and D.M. Strachan, *J. Crystal Growth* (in review).
18. J. Ito, *Amer. Mineral.* 53, 890 (1968).
19. J. Felsche, *J. Solid State Chem.* 5, 266 (1972).
20. J. Felsche, in *Structure and Bonding 13* (eds. J.D. Dunitz, P. Hemmerich, J.A. Ibers, C.K. Jørgensen, J.B. Neilands, R.S. Nyholm, D. Reinen, and R.J.P. Williams), Springer-Verlag, Berlin, p. 99-197 (1973).
21. D. McConnell, *Apatite: Its Crystal Chemistry, Mineralogy, Utilization, and Geologic and Biologic Occurrences.* Springer-Verlag, New York (1973).
22. R.C. Ewing, W.J. Weber, and F.W. Clinard, Jr., *Progress in Nuclear Energy* 29, 63 (1995).
23. W.J. Weber, R.C. Ewing, C.A. Angell, G.W. Arnold, A.N. Cormack, J.M. Delaye, D.L. Griscom, L.W. Hobbs, A. Navrotsky, D.L. Price, A.M. Stoneham, and M.C. Weinberg, *J. Mater. Res.* 12, 1946 (1997).
24. W.J. Weber, R.C. Ewing, C.R.A. Catlow, T. Diaz de la Rubia, L.W. Hobbs, C. Kinoshita, Hj. Matzke, A.T. Motta, M. Nastasi, E.H.K. Salje, E.R. Vance, and S.J. Zinkle, *J. Mater. Res.* 13, 1434 (1998).
25. W.J. Weber, R.P. Turcottte, and F.P. Roberts, *Radioactive Waste Mangement* 2, 295 (1982).
26. W.J. Weber and F.P. Roberts, *Nuclear Technology* 60, 178 (1982).
27. W.J. Weber, *Radiation Effects* 77, 295 (1983).

28. W.J. Weber, J. Amer. Cer. Soc. 76, 1729 (1993).
29. W.J. Weber, N.J. Hess, and L.M. Wang, Mat. Res. Soc. Symp. Proc. 321, 435 (1994).
30. L.M. Wang, M. Cameron, W.J. Weber, K.D. Crowley, and R.C. Ewing, in: *Hydroxyapatite and Related Materials* (eds. P.W. Brown and B. Constantz), CRC Press, p.243-249 (1994).
31. L.M. Wang and W.J. Weber, Phil. Mag. 79, 237 (1999).
32. M. Cameron, L.M. Wang, K.D. Crowley, and R.C. Ewing, in: *Proc. 50th Annual Meeting Electron Microscopy Soc. Amer.* (eds. G.W. Bailey, J. Bentley, and J.A. Small), San Francisco Press, p. 378-493 (1992).
33. W.J. Weber, R.C. Ewing, and A. Meldrum, J. Nucl. Mater. 250, 147 (1997).
34. W. Lutze, J. Borchardt, and A.K. De, in: *Scientific Basis for Nuclear Waste management I* (ed. G.J. McCarthy), Plenum Press, New York, p. 69-81 (1979).
35. P.J. Hayward, in: *Radioactive Waste Forms for the Future* (eds. W. Lutze and R.C. Ewing), North-Holland Physics Publishing, Amsterdam, p. 427-493 (1988).
36. P.J. Hayward, Glass Technology 29, 122 (1988).
37. I.W. Donald , B.L. Metcalfe, and R.N.J. Taylor, J. Mater. Sci. 32, 5851 (1997).
38. F. Bart, V. L'Hermite, S. Houpert, C. Fillet, F. Pacaud, and N. Jacquet-Francillon, 99th Annual Meeting Amer. Cer. Soc. (1997).
39. L.R. Morss, M.K. Richmann, and D. Lexa, Abstr. Pap. Amer. Chem. Soc. 218, p. 99-IEC (1999).
40. V.M. Oversby, in: *Materials Science and Technology: A Comprehensive Treatment 10B (Nuclear Materials, Part 2)* (ed. B.R.T. Frost), VCH, Weinheim, p. 391-442 (1994).
41. M.E. Fleet and Y. Pan, Amer. Mineral. 80, 329 (1995).
42. H.J. Forster HJ, Amer. Mineral. 83, 1302 (1998).
43. R. Bros , J. Carpena, V. Sere, and A. Beltritti, Radiochimica Acta 74, 277 (1996).
44. Meis et al., J. Appl. Chem. A 104, 5380 (2000).